Kinetics of the Reactions of NO3 Radical with alkanes

Li Zhou, A R Ravishankara, Steven S Brown, Kyle J Zarzana, Mahmoud Idir, Véronique Daële, Abdelwahid S Mellouki

Kinetics of the Reactions of NO_3 Radical with alkanes

Li Zhou,[a,g] A.R. Ravishankara,[a,b,c,*] Steven S. Brown,[d,e] Kyle J. Zarzana,[d,f,h] Mahmoud Idir,[a] Véronique Daële,[a] Abdelwahid Mellouki[a,*]

a. Institut de Combustion, Aérothermique, Réactivité et Environnement/OSUC, CNRS, 45071 Orléans Cedex 02, France

b. Departments of Chemistry and Atmospheric Science, Colorado State University, Fort Collins, CO 80253, USA

c. Le Studium Loire Valley Institute for Advanced Studies, Orléans, France.

d. NOAA Earth System Research Laboratory (ESRL) Chemical Sciences Division, 325 Broadway, Boulder, CO 80305, USA

e. Department of Chemistry, University of Colorado Boulder, Boulder, CO 80309, USA

f. Cooperative Institute for Research in Environmental Sciences, University of Colorado Boulder, Boulder, CO 80309, USA

g. Now at: National Engineering Research Center for Flue Gas Desulfurization, Department of Environmental Science and Engineering, Sichuan University, Chengdu, 610065, China

h. Now at: Department of Chemistry, University of Colorado Boulder, Boulder, CO 80309 USA.

*Address correspondence to:

A.R.Ravishankara@colostate.edu or mellouki@cnrs-orleans.fr

Abstract

The rate coefficients for the reactions of NO_3 radicals with methane (CH_4), ethane (C_2H_6), propane (C_3H_8), n-butane (n-C_4H_{10}), iso-butane (iso-C_4H_{10}), 2,3-dimethybutane (C_6H_{14}), cyclopentane (C_5H_{10}) and cyclohexane (C_6H_{12}) at atmosphere pressure (1000±5 hPa) and room temperature (298±1.5 K) were measured using an absolute method. Careful attention was paid to the role of secondary reactions and impurities. The upper limits of rate coefficients for methane and ethane at 298 K are $<4 \times 10^{-20}$ and $<5 \times 10^{-19}$ cm^3 $molecule^{-1}$ s^{-1}, respectively. The rate coefficients at 298 K for propane, n-butane, iso-butane, 2,3-dimethybutane, cyclopentane and cyclohexane are, $(9.2\pm2.9) \times 10^{-18}$, $(1.5\pm0.4) \times 10^{-17}$, $(8.2\pm2.2) \times 10^{-17}$, $(5.8\pm2.4) \times 10^{-16}$, $(1.5\pm0.6) \times 10^{-16}$ and $(1.3\pm0.4) \times 10^{-16}$ cm^3 $molecule^{-1}$ s^{-1}, respectively. Rate coefficients for the reactions of NO_3 radical with two deuterated n-butanes (butane-D10 and butane-1,1,1,4,4,4-D6) are also reported. We show that the rate coefficients for NO_3 reactions correlate with the enthalpy change for the reaction, thereby suggesting that the mechanism for NO_3 reactions with alkanes is through H atom abstraction. The measured rate coefficients are compared with available literature values. This study increases the number of available rate coefficients for the reactions of NO_3 with alkanes and sets significantly lower upper limits for reaction of NO_3 with ethane and methane. The atmospheric significance of our reported rate coefficients is briefly discussed.

1 Introduction

Alkanes are ubiquitous in the Earth's atmosphere and come from both natural and anthropogenic sources. They play many important roles in the atmosphere: (a) they are precursors for tropospheric ozone; (b) they contribute to secondary organic aerosol formation; (c) they are important reactants for removal of free radicals such as OH, Cl, and possibly NO_3 radicals; and (d) the longer-lived alkanes are also a source of stratospheric water vapor. Methane is the second most important anthropogenic greenhouse gas and estimates of its radiative forcing depend on accurate assessment of its atmospheric lifetime. Therefore, an accurate characterization of the loss rates of alkanes to reaction with major atmospheric oxidants, including NO_3, is important. Also, their role in the removal of NO_3 needs quantification.

Most alkanes are removed from the atmosphere via their reactions with the ubiquitous OH radical, with minor contributions from reactions with Cl atoms. Reactions of alkanes with ozone are too slow to be significant. However, NO_3 radical may also contribute to their removal under special conditions and, more importantly, the alkanes may substantially contribute to the removal of the NO_3 radicals. This is especially the case with more reactive large alkanes. For example, Wild et al.[1] showed that alkanes contributed roughly 45%-50% of the gas phase NO_3 loss rates in an oil and gas basin where alkanes were the dominant class of VOC. This analysis was based on available literature at that time, including upper limits for some reactions.

The rate coefficients for the reactions of alkanes with NO_3 radicals are relatively small and they have not been subject to extensive examinations unlike the case of OH radical and Cl atom reactions. Mostly, large upper limits at room temperature have been reported for the reactions of NO_3 with methane, ethane, and propane. Furthermore, most of these measurements have been derived from relative rate measurements methods. Suitable reference compounds with well-established small reaction rate coefficients are difficult to find and hence the reported rate coefficients are likely to have significant uncertainties. The rate coefficients for the reactions of NO_3 with larger alkanes, which

react more rapidly, have been reported; however, there are large variations amongst even the few reports.[2-5] Therefore, further investigations of the rate coefficients for the reactions of NO_3 with simple alkanes are needed.

In this study, we have utilized a direct method developed recently in our laboratory to measure NO_3 reaction rate coefficients that is well-suited for slow reactions. We have employed this method to measure the rate coefficients for the following reactions at (298±1.5) K with the Δ_rH^o(298 K) noted next to the reaction:

$NO_3 + CH_4$ (methane) $\rightarrow CH_3 + HNO_3$; +15.12 kJ mol^{-1} (1)

$NO_3 + C_2H_6$ (ethane) $\rightarrow C_2H_5 + HNO_3$; -2.44 kJ mol^{-1} (2)

$NO_3 + C_3H_8$ (propane) $\rightarrow$ n-$C_3H_7 + HNO_3$; -0.74 kJ mol^{-1} (3a)

$NO_3 + C_3H_8$ (propane) $\rightarrow$ iso-$C_3H_7 + HNO_3$; -10.74 kJ mol^{-1} (3b)

NO_3 + n-C_4H_{10} (n-butane) $\rightarrow$ 1-C_4H_9 (1-Butyl) + HNO_3; +0.65 kJ mol^{-1} (4a)

NO_3 + n-C_4H_{10} (n-butane) $\rightarrow$ 2-C_4H_9 (2-Butyl) + HNO_3; -10.84 kJ mol^{-1} (4b)

NO_3 + iso-C_4H_{10} (iso-butane) $\rightarrow C_4H_9$ (Isobutyl) + HNO_3; -1.24 kJ mol^{-1} (5a)

NO_3 + iso-C_4H_{10} (iso-butane) $\rightarrow C_4H_9$ (t-butyl) + HNO_3; -23.24 kJ mol^{-1} (5b)

$NO_3 + C_6H_{14}$ (2,3-dimethybutane) $\rightarrow C_6H_{13}$ (2,3-dimethyl -1-Butyl) + HNO_3;

$\approx$ 12 kJ mol^{-1} (6a)

$NO_3 + C_6H_{14}$ (2,3-dimethybutane) $\rightarrow C_6H_{13}$ (2,3-dimethyl -2-Butyl) + HNO_3;

-34.64 kJ mol^{-1} (6b)

$NO_3 + C_5H_{10}$ (cyclopentane) $\rightarrow C_5H_9$ (cyclopentyl) + HNO_3;

-23.98 kJ mol^{-1} (7)

$NO_3 + C_6H_{12}$ (cyclohexane) $\rightarrow C_{12}H_{11}$ (cyclohexanyl)+ HNO_3;

-26.84 kJ mol^{-1} (8)

The enthalpy of each reaction was calculated by using the respective Δ_fH^o(298 K) values from NIST Standard Reference Database.[6] The enthalpy change for reaction (6a) was estimated assuming the C-H bond strength to be similar to that in reaction (5a). Enthalpy change for reaction (6b) was obtained using data from Baldwin et al.[7]

We monitored the temporal profiles of NO_3 (and N_2O_5 that is in equilibrium with

NO_3) using a cavity ring down spectrometer over a time scale of 10-20 minutes in an excess of alkanes at a total pressure of (1000±5) hpa in a large chamber to directly determine the rate coefficients.

2 Experimental section

The experimental set up and the procedure used has been described in detail in a previous publication.[8] The rate coefficients for reactions (1-8) were measured by following the temporal profiles of NO_3 and N_2O_5 in an excess of each alkane. The concentrations of NO_3 and N_2O_5 were both measured via cavity ring down spectroscopy. The reactions were carried out in a large chamber that allowed measurement of the slow loss of the NO_3 and N_2O_5 over long periods of time (up to 30 mins). Here, we will briefly describe the experimental set up, the analytical instruments used to quantify alkanes, NO_3, N_2O_5, and NO_2, and the data acquisition procedures.

2.1 Experimental system

The rate coefficients were measured at room temperature (298.0±1.5K) in the ICARE-7300L dark Teflon chamber at slightly above the ambient pressures (1000±5hpa).[9, 10] Before each set of experiments, the chamber was flushed overnight with dry zero air (relative humidity <3%) to remove alkanes and nitrogen oxides to below their detection limits (see below). The gaseous reactants were flowed into the chamber from a gas handling system where mixtures were made using calibrated capacitance manometers (0-10, 0-100 and 0-1000 Torr, MKS Baratron). The larger alkanes, which are liquids, were evaporated into glass bulbs where their pressures were measured and then filled with dry air to known pressures. A measured pressure of this mixture was introduced into a calibrated volume and then this gas mixture was flushed into the chamber using zero air.

All the analytical instruments sampled from the middle of the chamber. The

temperature in the chamber was measured using two thermocouples located in different parts of the chamber; they were the same to within 0.5 K and remained constant during the rate coefficient measurements. The pressure in the chamber was measured using a capacitance manometer.

A small flow (about 10 L/min) of purified air was added to make up for the continuous withdrawal of gases for analysis from the chamber and keep the pressure constant. This procedure slowly diluted the chamber contents. The contents of the chamber were mixed by two internal fans. We measured the time constants for these two processes, dilution and mixing, by adding a sample of SF_6 (>99.99%, Alpha Gaz) into the chamber and following its temporal profile using an FTIR spectrometer (see below). The dilution rate could be expressed as a first order loss with a rate coefficient of $(2.5 \pm 0.1) \times 10^{-5}$ s^{-1} (as shown in Figure S1, in the supporting information section) and the mixing time (for >99% mixing) was (30±3) seconds.

The contents of the chamber were sampled using: (a) an FT-IR spectrometer to measure hydrocarbon concentrations; (b) a cavity ring down spectrometer to simultaneously measure NO_3 and N_2O_5; and (c) a Cavity Attenuated Phase Shift (CAPS) spectroscopy instrument to measure NO_2. They are described below. The IR absorption bands of methane were partially saturated because of the large the concentrations used in our study. Therefore, methane concentrations in the chamber were determined manometrically. This approach was very accurate since we could directly measure the substantial pressure of methane that was introduced into the chamber.

(a) *FT-IR spectrometer*: A commercial Nicolet 5700 Magna FT-IR spectrometer with a liquid nitrogen cooled mercury–cadmium–telluride (MCT) detector was coupled to a white-type multiple-reflection mirror system located near the center of the chamber. The multipass system had a base path length of 2 m and, with 70 traverses, a total optical path length of 140 m. The spectra, measured between 4000–700 cm^{-1}, were analyzed using the software provided by the vendor (OMNIC 9). The IR spectra were recorded in 63s by co-adding 16 scans at a spectral resolution of 1 cm^{-1}. The alkanes and SF_6 were monitored at the following wavenumbers: ethane (940-734 cm^{-1}), pentane (1576-

1298 cm^{-1}), n-butane (3083-2798 cm^{-1}), iso-butane (3053-2808 cm^{-1}), cyclopentane (3100-2800 cm^{-1}), cyclohexane (2970-2830 cm^{-1}), 2,3-dimethy butane (3035-2821 cm^{-1}) and SF_6 (934- 954 cm^{-1}).

The integrated absorbances, the areas under the curves of the measured absorbances with absorption wavenumbers noted above, were used to determine concentrations. Calibration plots were generated by plotting the integrated absorbance against known mixing ratio of the hydrocarbon (ppmv); an example for ethane is shown in Figure 1. Similar plots for other alkanes are shown in the supporting information (Figure S2).

(b) *Cavity Ring Down Spectrometer*: A two-channel cavity ring down spectrometer operating at 662 nm was used to simultaneously measure the concentrations of NO_3 (in one channel) and N_2O_5 + NO_3 (in another channel). The operating characteristics of this instrument have been described in detail elsewhere.[11-14] The time resolution of the instrument was 1s with detection limits of 0.4 and 2 pptv, respectively, for NO_3 and N_2O_5 for 1 second integration as described in detail by Fuchs et al.[15] The sample from the chamber entering the CRDS system was passed through a filter to remove aerosols, which scatter the 662 nm light and thus degrade the sensitivity for NO_3 detection. The losses of NO_3 and N_2O_5 to the walls of the instrument and the filter assembly have been estimated[15-18] to be less than 20% and 4%, respectively; these losses were accounted for in calculating the concentrations. The overall accuracy of the measured NO_3 and N_2O_5 concentrations, respectively, are estimated to be from -8% to +11% and from −9% to +12%.[14] In the current study, the NO_3 and N_2O_5 mixing ratios were, respectively, between 50 and 2,500 pptv and between 1,000 and 28,000 pptv. The precisions of these measurements are much better than the quoted absolute uncertainties under the concentration conditions used in the present study. Therefore, the temporal variation of these reagents could be determined very precisely.

(c) *The CAPS instrument*: A commercial NO_2 monitor from Aerodyne Research Inc. was used to measure the NO_2 concentrations during the experiments. This instrument measures absorption due to nitrogen dioxide at 450 nm using cavity

attenuation that is detected by phase shift measurements. Levels of detection (3σ noise levels), as specified by the vendor, was less than 100 pptv for a 10 second averaging period.[19]

2.2 Chemicals

The following chemicals, with purities as stated by the supplier, were used without further purification: methane (> 99.995%, Air Liquid), ethane (> 99.995%, Air Liquid), propane (> 99.95%, Air Liquid), iso-butane (> 99.95%, Air Liquid), n-butane (> 99.95%, Air Liquid), cyclopentane (> 99.5%, Aldrich), cyclohexane (>99.5%, Aldrich), 2,3-dimethy butane (>99.5%, Aldrich), n-butane-D10 (98 atom % D, Aldrich) and n-butane-D6 (98 atom % D, Aldrich) . The alkene impurities in these samples are important since they can influence the measured rate coefficients. Therefore, they were measured using GC-MS analyses and are noted elsewhere.

The NO_3 radicals were produced by thermal decomposition of N_2O_5 injected into the chamber. Pure N_2O_5 was synthesized by mixing NO to a slowly flowing mixture of O_3 in N_2 and collecting N_2O_5 in a trap at 193 K. The collected N_2O_5 was purified via trap-to-trap distillation, as described by Davidson et al.[20]

2.3 Kinetic study method

The rate coefficients for the reactions of NO_3 radicals with alkanes were measured by following the temporal profiles of NO_3, N_2O_5 and NO_2 in excess of alkanes. During this process, NO_3, N_2O_5 and NO_2 are in equilibrium; therefore, the loss of NO_3 also leads to the loss of N_2O_5. The temporal profiles of the absolute concentrations of the NO_3 and/or N_2O_5 can then be fit to a kinetic model to extract the reaction rate coefficient of interest, as explained previously.[8]

N_2O_5 was injected into the middle of the chamber, where it decomposed to give NO_3 and NO_2 and rapidly set up equilibrium amongst these species.

$N_2O_5 \xrightarrow{k_9} NO_3+NO_2$ (9)

$NO_3+NO_2 \xrightarrow{k_{10}} N_2O_5$ (10)

The temporal variations of the concentrations of NO_3, N_2O_5 and NO_2 in the chamber were continuously measured. The concentrations of NO_3 and N_2O_5 decreased with time as NO_3 reacted with the alkanes and both N_2O_5 and NO_3 were lost to the walls of the chamber. The measured temporal profiles of NO_3, N_2O_5 and NO_2 concentrations were calculated using a box model that integrated the set of reactions occurring in the chamber. The calculated profiles were compared to the observed concentrations and the differences between the observed and calculated concentrations were minimized (using a non-linear least squares algorithm). The fitting was done by minimizing together the sum of least-squares for both NO_3 and N_2O_5 profiles while changing the input parameters. The input parameters included the initial concentrations of each reactant (as measured) and rate coefficients for the reaction of NO_3 with alkanes. First, the data in the absence of alkane (the first 10 mins after N_2O_5 injection and before the injection of alkanes) were fit to the reaction scheme with alkane concentration set to zero using the known values of k_9 and k_{10} from NASA/JPL recommendation.[21] (The derived rate constants for NO_3 + alkane were not very sensitive to the choice equilibrium constants used; the difference between using the IUPAC versus NASA/JPL value for the equilibrium constant yielded rate coefficients that were less than 5% different.) The values of the first order rate coefficients for loss of NO_3 and N_2O_5 to the walls (k_{11}, s^{-1} and k_{12}, s^{-1}) were derived from the fit of the reaction scheme shown below:

$N_2O_5 \xrightarrow{k_9} NO_3+NO_2$ (9)

$NO_3+NO_2 \xrightarrow{k_{10}} N_2O_5$ (10)

$NO_3 \xrightarrow{k_{11}} \text{loss}$ (11)

$N_2O_5 \xrightarrow{k_{12}} \text{loss}$ (12)

Subsequently (roughly 10 mins after N_2O_5 injection), a known concentration of the alkane was introduced into the chamber to allow NO_3 to react with the alkane of interest:

NO_3 + alkane $\xrightarrow{k_x}$ products (R_1+HNO_3) (1-8)

The concentration of the alkane was measured using the FTIR (or pressure in case of CH_4). As shown in Table 2 and 3, the concentration of the alkane was always at least a 2000 times (often hundreds-of-thousands of times) greater than that of NO_3 in the chamber. The temporal profiles of N_2O_5, NO_3 and NO_2 measured 60 s (roughly double the time it takes for complete mixing) after alkane injection were again fit to the above reaction scheme that includes Reaction (1-8). Again, the fitting was done by minimizing the sum of least-squares for NO_3 and N_2O_5 decays in the reaction scheme by varying only the rate coefficient for the reaction of alkanes; the values of k_{11} and k_{12} were fixed to the values derived from the observation in the absence of alkanes (i.e., during the first ~10 mins). The initial NO_2 concentrations were sometimes altered very slightly (less than 10%, well within the uncertainty of our measurements) to make the equilibrium constant derived from our observations agree with the known equilibrium constant from NASA/JPL evaluations. Part of this discrepancy could be due to a small amount of N_2O_5 decomposing in the CAPS instrument and the resultant NO_2 and NO_3 being detected at 450nm. Tests showed that the NO_2 concentration could be utmost 15% lower than that measured by CAPS due to the potential interference due to concentration of N_2O_5 in the chamber. We note that NO_2 concentration was not central to our analysis to obtain the rate coefficients.

3 Results and discussion

3.1 Accounting for subsequent reactions and impurities

We studied Reactions (1) through Reaction (8) under pseudo-first order conditions in NO_3 in the presence of an excess of alkanes. The temporal profiles of NO_3 depends on: 1) the reaction under study; 2) its equilibrium with N_2O_5; and 3) the quantified dilution and wall losses. Figure 2 shows the observed temporal profiles of NO_3, N_2O_5,

and NO_2 for Reaction (1).

Many of the reactions studied here are very slow and we encountered two difficulties that needed to be accounted for: (1) the temporal profiles of NO_3 (and N_2O_5) could be influenced by its subsequent reactions with the products of the initial reaction; and (2) we needed to quantify the contribution of the reactive impurities (mostly alkenes, if present) in the excess reagent because their presence could lead to an overestimation of the rate coefficients. To examine and account for interferences due to secondary reactions, we carried out a series of calculations using a box model that contained the reactions in Table 1. We initially used a larger set of reactions that could take place in the chamber and found that the NO_3 profiles were controlled by the subset of reactions shown in Table S1. To examine the influence of impurity reactions, we analyzed the reactants for the presence of impurities and examined the dependence of the measured rate coefficients as a function of reaction time. As shown later, if there were very small amounts of impurities that could still influence the measured rate coefficients, they should be reacting away with NO_3 in the initial period and thus we should see a dependence of the measured rated coefficients with reaction times. This point will be discussed later.

Table 1

3.2 Experimental results

Figure 2 shows the observed and simulated temporal profiles of NO_3, N_2O_5, and NO_2. Simulated profiles were obtained by numerical integration of the mechanism shown in Table 1, as discussed above. Panel (1) shows these losses in the absence of methane with the methane concentration set to zero. From this fit, the rate coefficients for the wall loss of NO_3 and N_2O_5 were derived. Panel (2) shows the loss of NO_3 and N_2O_5 in the presence of 2647 ppmv of methane. These data were again fit using the mechanism in Table 1 with all of the rate coefficients for the secondary reactions set to zero, i.e., the additional NO_3 loss attributed to only reaction with methane. Panel (3) shows the same data as in panel 2, but the fits included all the reactions shown in Table

1. Clearly, the fits in panel 2 and 3 are both good, but the obtained values of the rate coefficient for the reaction of NO_3 with CH_4 are different. The reason for the good fit in both cases is that the reactions subsequent to initial reaction with CH_4 are rapid and have the effect of changing the stoichiometry from 1 to 2, or more, for NO_3 radicals consumed per reaction with methane.

Figure 2

Multiple experiments were carried out by varying concentration of alkanes and initial NO_3. The fits of the observed temporal profiles in such experiments for ethane are shown in the supporting information as Figure S3. The inclusion of secondary reactions in the simulations shows that they contribute substantially to the measured temporal profiles and derived NO_3 reaction rate coefficients.

Table 2

We examined the ratios of the rate coefficient obtained without and with the inclusion of the secondary reactions (Ratio 1) as a function of the ratios of the alkane to initial NO_3 concentrations (Ratio 2) (Figure 3). Clearly, the Ratio 1 decreased as the ratio of the methane/ethane to NO_3 (Ratio 2) increased. It asymptotically approached 1, as the ratio of alkane to NO_3 increased. Ideally, an additional factor of 10 increase in the alkane to NO_3 ratio would have almost completely suppressed the importance of the secondary reactions. However, such a ratio was difficult to achieve in our chamber. Increasing the alkane concentration would increase the NO_3 loss rate relative to the mixing time and possibly perturb the equilibration between NO_3 and N_2O_5. Decreasing the NO_3 concentration would decrease the precision of measured NO_3 profiles (measured for approximately 20 minutes).

Figure 3

The presence of any reactive impurity whose concentration does not change appreciably with reaction time will not be sensitive to this analysis and could influence the accuracy of the measured rate coefficient. The effects of reactive impurities are discussed further in the section on error estimation below.

3.3 Measured rate coefficients and their uncertainties

The results of our measured values of k_1-k_8 are given in Tables 2 and 3. We will first discuss the estimated uncertainties in these reported rate coefficients.

Table 3.

The errors on the reported rate coefficients arise from: (1) the precision in the measurements of the concentrations of NO_3, N_2O_5 and NO_2; (2) the uncertainty in the concentration of the alkanes, the excess reagent; (3) the uncertainty of the rate coefficients shown in Table 1; and (4) the precision of our fitting.

In the present study, the systematic errors in measurements of NO_3 and N_2O_5 using the CRDS system employed here have been assessed to be −8/+11% for NO_3 and −9/+12% for N_2O_5, as noted earlier. The error in measurement of NO_2 (after correcting for the potential interference due to N_2O_5) using CAPS monitor has been assessed to be 15%. Systematic errors in the measured concentration of the alkanes are estimated to be 5% for each compound (this includes the uncertainties in the calibration curves that is mostly due to the manometric preparation of the mixtures and the uncertainties in measuring the integrated absorbance). All the noted uncertainties are at the 95% confidence level. The uncertainty in the fitting, as noted above, is better than 5%. But the uncertainty of the rate coefficients used in the reaction scheme of the box model to fit the curves (k_7, k_8) can reach almost 60%.[22] This uncertainty includes estimated error arising from not simulating the entire reaction sequence. Note that this uncertainty does not translate linearly into the estimated uncertainties in the rate coefficients. For example, an uncertainty of 50% in the rate coefficients for the reaction of RO_2 with NO_3, the major secondary reaction, translates to an uncertainty of less than 15% in the reported value of the rate coefficient. Therefore, we estimated that the uncertainty in our simulated correction is less than 15% for the uncertainty in this rate coefficient. To be conservative, we have used the larger uncertainties in calculating the upper limits for k_1 and k_2.

The uncertainty in the obtained value of k_{alkane} due to fitting was typically less than

7%. The uncertainty in the precision of our measured rate coefficients were obtained by the standard deviation of the mean of multiple measurements and including the Student t value accounting for the limited number of measurements. The overall estimated error in the rate coefficients included the fitting error, estimated uncertainty of absolute concentrations of each reactant, the precision of the measurements of k_{alkane}, and the uncertainty due to potential errors in the rate coefficients used from the literatures into account.

Another potential source of error in the rate coefficients measured by using the absolute method is the presence of reactive impurities in the sample of the alkanes. The alkanes used in the study were the purest we could obtain from commercial vendors. For methane and ethane, the impurities are less than 0.005% (50 ppmv) and the main impurities are nonreactive gases such as, N_2, O_2, and CO_2. However, we cannot rule out very small amounts of reactive impurities (<20 ppm). If such an impurity that reacts with a rate coefficient of 1×10^{-13} cm^3 $molecule^{-1}$ s^{-1} were present, its concentration cannot be more than about 0.5 ppmv even if we attributed the entire measured rate coefficient to the impurity reaction. For methane and ethane, second and third aliquots of N_2O_5 (~20 ppbv) were introduced to the chamber roughly 1 hour after the initial alkane injection. Small amounts of reactive impurities would have reacted with NO_3 over the hour, reducing their concentrations. The temporal profiles of NO_3, N_2O_5 and NO_2 were again fit to the reaction scheme and we obtained rate coefficient (k_{alkane}) that were within 7% of the initial values, a difference significantly smaller than the estimated uncertainty. Therefore, from these experiments, we estimate that less than 0.1 ppmv reactive impurities were present in the alkane samples. Based on these observations, we suggest that the contribution of reactive alkenes was small. It is still possible that the reaction of NO_3 with methane and ethane could be slower than the values noted above. Therefore, we quote the rate coefficients for the reactions of NO_3 with methane and ethane to be upper limits of, respectively, $<4\times10^{-20}$ and $<5\times10^{-19}$ cm^3 $molecule^{-1}$ s^{-1}.

Gas chromatography- mass spectrometry (GC-MS) was used to measure the levels

of olefinic impurities in propane, n-butane and iso-butane. Our detection limit for alkenes in these alkanes was < 20ppmv. For propane, less than 50 ppm propene was detected as a main reactive impurity, and mixing ratios for other olefins were below the detection limit of 20 ppmv. Based on these upper limits for olefins, we conclude that our measured values for k_3-k_5 were not influenced by alkenes.

Figure 4

The rate coefficient for reaction of propane with NO_3 radicals was obtained by fitting the observed temporal profiles of NO_3, N_2O_5, NO_2 in different conditions as shown Figure 4. Simulation of these profiles where we assumed 50 ppmv of propene impurity in propane are shown as the line in Figure 4. Based on such simulations, we estimate that effect of reactive impurity to the reaction rate coefficient for NO_3 reaction with propane is less than 7%. Furthermore, fits to the data from different reaction time periods, when some of the alkenes should have been depleted due to reaction with NO_3, yielded rate coefficients that were less than 10% different. However, the simulations show that 50 ppmv of propene would not be completely remove by the levels of NO_3 present in the reactor.

The rate coefficients for reaction of NO_3 with n-butane, iso-butane, 2,3-dimethylbutane cyclopentane and cyclohexane were also studied in this work, and the typical observed temporal profiles of NO_3 and N_2O_5 in such experiments are similar to those of other alkanes described above. The purities of each alkane specified by the vendor and determined by GC-MS measurements are listed in Table S2. The contributions of this level of olefins in alkanes do not affect the measured rate coefficient by more than 10%. The related Figure S4 in the supporting information demonstrates the derivation of the same rate constant at different reaction times for the NO_3 + cyclopentane system. The experimental conditions and rate constants for reaction of NO_3 with these reactants are summarized in Table 3. The related figures are shown in the Supporting Information as Figure S5-Figure S9.

The results in Table 3 clearly shows that a major contributor to the uncertainty in our measured rate coefficients is the secondary reactions of NO_3 with the products of

the reactions noted earlier. This uncertainty has been incorporated in our analyses.

3.4 Comparison with the kinetic results in literature

Many of the reported rate coefficients for alkanes were measured relative to that of NO_3 with ethene. The rate constant of ethene with NO_3 was recommended by IUPAC[22] to be $(2.1 \pm 1.2) \times 10^{-16}$ cm^3 molecule^{-1} s^{-1}; i.e., with an uncertainty of 58% uncertainty. Therefore, we measured the rate coefficient for this reaction using the same method as for alkanes to be $(2.6\pm0.4) \times 10^{-16}$ cm^3 molecule^{-1} s^{-1} (see Supplementary Table S3). We used our measured value to place previous relative measurements on an absolute basis.

Our measured rate coefficients of NO_3 radicals with alkanes are compared with those from the literature in Table 4. The upper limits of methane with NO_3 radicals were all derived based on no observable reaction occurring in their systems.[5, 28-30] The results of Cantrell et al[30] on k_1 are very indirect and is based on their inability to detect CO and CO_2 in their reactor when CH_4 was mixed with NO_3 and N_2O_5. It is possible that the reactions of CH_3 radicals in their system could lead to end-products other than CO or CO_2, e.g., nitrates or formaldehyde. The upper limits for k_2 at room temperature were derived by Wallington et al and Boyd et al to be $<2.7\times10^{-17}$ and $<4\times10^{-18}$ cm^3 molecule^{-1} s^{-1}, respectively.[5, 24] Bagley et al.[4] reported k_2 at 453K and above. An extrapolation of their measured rate coefficients using the Arrhenius expression leads to k_2 (298K) = 2.0×10^{-18} cm^3 molecule^{-1}s^{-1}, and but likely has a significant uncertainty. Previous studies have obtained rate coefficients for reactions with n-butane are all higher than the value measured by all but Wallington et al.[29] We assume that Wallington et al. supersedes the earlier reported value from the same group.[2] It is likely that the difference with our value reported by Bagley et al is due to the extrapolation from high temperatures (where they measured the rate coefficients). The previous reported rate coefficients for the reactions with iso-butane and 2,3-dimethybutane at room temperature, mainly using relative rate techniques with ethene as the reference compound, are in good agreement with our values. In those cases, we recommend a weighted average (Table 4) for use in atmospheric calculations. There are no previous reports for the rate coefficients for the

reactions of NO_3 with cyclepentane. It is worth noting that agreement is better with larger alkanes with larger rate coefficients.

Table 4

Our upper limit for the reactions of NO_3 with methane is lower than all the previous reports except for that by Cantrell et al. As noted earlier, the upper limit reported by Cantrell et al. was based on the absence of CO and CO_2 being produced in their system. The low rate coefficient for this reaction is not surprising since it is slightly endothermic, and the barrier height for the reaction is large. We also report an upper limit for the reaction of NO_3 with ethane, lower than all previous reports. We quote this only as an upper limit given that it is very low and very small levels of impurities can lead to errors.

We are the first to report, to the best of our knowledge, the rate coefficients of NO_3 reaction with propane and cyclopentane. The reported values of the rate coefficients of 2,3-dimethylbutane and cyclohexane are in reasonable agreement with available values. A weighted average of these values (Table 4) is recommended for atmospheric purposes.

3.5 Relation between structure and reactivity of alkanes.

We observe an increase in the reactivity with the chain length k_1(methane) < k_2(Ethane) < k_3(Propane) < k_4(n-butane). Further, the iso-butane and 2,3-dimethybutane react faster than their normal analogs. This observation is consistent with NO_3 reaction occurring via H atom abstraction from primary, secondary, and tertiary C-H bonds, respectively.

For simple alkanes, the C-H bond dissociation energies are: primary C-H, -100 kcal mol^{-1}; secondary C-H, -96 kcal mol^{-1} and tertiary C-H -94 kcal mol^{-1}, respectively.[31] So, we expect the reaction to be faster for molecules with lower C-H bond energy, since we expect the reaction to proceed via H atom abstraction from the weakest C-H bonds in the molecule.

To further examine this mechanism, the rate coefficients for reactions of NO_3 with two different deuterated n-butanes (n-butane-d10 and n-butane-1,1,1,4,4,4-d6) were measured (see Table 5) to be $(7.4 \pm 2.3) \times 10^{-18}$ and $(2.0 \pm 0.5) \times 10^{-17}$ cm^3 $molecule^{-1}s^{-1}$,

respectively. Because of possible reactive impurities in the gas samples, the rate coefficients obtained for n-butane-d10 and n-butane-1,1,1,4,4,4-d6 may be overestimates. As seen from these values, k_4(n-butane)/$k_{(n\text{-butane-d6})} > 0.75$, and k_4(n-butane)/$k_{(n\text{-butane-d10})} > 2$. Therefore, deuteration reduces the rate coefficient for the reaction, an observation consistent with a reaction mechanism via H atom abstraction.[32,33]

Table 5.

The enthalpies of each reaction under standard state conditions are shown in the introduction section. From the enthalpies of these reactions, we find Reaction (1) and (4a) to be endothermic reactions and all the other reactions are exothermic.

We have plotted the rate coefficient for the measured alkanes and cycloalkanes as a function of the reaction exothermicity (Reaction (1), (2), (3), (4b), (5b), (6b), (7) and (8)) in Figure 5. Clearly, the log of the rate coefficient at 298 K correlates with the exothermicity or the bond dissociation energy. This is to be expected for an abstraction reaction where the activation energy for the reaction is directly related to the dissociation energy for the bond being broken, i.e., the C-H bond in the reactions studied here. The correlation is surprisingly robust. Based on this correlation, we suggest that the rate coefficient for the reaction of NO_3 with CH_4 is not more than a factor of five lower than that reported here. Also, this correlation and the finding that the reaction proceeds via H atom abstraction from the weakest C-H bond mean that reactions 1-8 will have substantial activation energies. Therefore, one would expect the rate coefficients to be smaller at lower atmospheric temperatures.

Figure 5.

4 Atmospheric implication

Calculation of the atmospheric lifetimes of VOCs, including alkanes, due to their reaction with NO_3 is difficult since neither NO_3 nor larger alkanes are uniformly mixed in the troposphere[34]. The reactions of NO_3 with smaller alkanes are clearly negligible. Lifetime comparisons for VOCs by reaction with different oxidants can be estimated

using the following equation[35].

$$\tau = \frac{1}{k_{voc}[X]}$$

In this calculation, [X] represents the concentration of typical atmospheric oxidants (OH, Cl and NO_3) and k_{alkane} is the rate constant of the reactions between alkanes and oxidants at 298 K. The concentrations for the oxidants vary greatly in the troposphere. For example, the measured range of NO_3 mixing ratios is 0.1 – 400 pptv. The estimated concentrations[36] of Cl atoms are usually less than 1×10^4 molecules cm^{-3}. The concentrations of OH radicals vary from essentially zero to roughly 10^7 cm^{-3}. Therefore, clearly, the contributions of NO_3 reactions towards the removal of alkanes will be negligible compared to those via OH radical or Cl atoms. Unlike OH and Cl atoms, NO_3 is prevalent at night. Therefore, one might expect that at high latitudes during long period of darkness the reactions of NO_3 with large alkanes could contribute to the removal of such alkanes. However, we expect the lower temperatures would also mean lower reactivities. Removal of large alkenes by NO_3 reactions has been suggested by Carslaw et al.[37] To our knowledge, there is no atmospheric evidence for significant removal of alkanes by NO_3. However, these NO_3 reactions could indeed contribute to the removal of NO_3 in regions with high alkane concentrations and temperatures closer to 298 K, such as in the regions affected by oil/gas extraction activities.[1]

Acknowledgment

This work was supported by the Labex Voltaire (ANR-10-LABX-100-01), ARD PIVOTS program (supported by the Centre-Val de Loire regional council), the European Union's Horizon 2020 research and innovation programme through the EUROCHAMP-2020 Infrastructure Activity under grant agreement No. 730997 and by the French National program LEFE (Les Enveloppes Fluides et l'Environnement). ARR was supported by Le Studium of the Loire Valley during his summer stay at CNRS-ICARE. SSB was supported by National Oceanic and Atmospheric Administration.

References

1. R. J. Wild, P. M. Edwards, T. S. Bates, R. C. Cohen, J. A. de Gouw, W. P. Dubé, J. B. Gilman, J. Holloway, J. Kercher, A. R. Koss, L. Lee, B. M. Lerner, R. McLaren, P. K. Quinn, J. M. Roberts, J. Stutz, J. A. Thornton, P. R. Veres, C. Warneke, E. Williams, C. J. Young, B. Yuan, K. J. Zarzana and S. S. Brown, *Atmos. Chem. Phys.*, 2016, **16**, 573-583.
2. R. Atkinson, C. N. Plum, W. P. Carter, A. M. Winer and J. N. Pitts Jr, *The J. Phys. Chem.*, 1984, **88**, 2361-2364.
3. R. Atkinson, S. M. Aschmann and J. N. Pitts Jr, *J. Phys. Chem.*, 1988, **92**, 3454-3457.
4. J. A. Bagley, C. Canosa-Mas, M. R. Little, A. D. Parr, S. J. Smith, S. J. Waygood and R. P. Wayne, *J. Chem. Soc., Faraday Trans*, 1990, **86**, 2109-2114.
5. A. A. Boyd, C. E. Canosa-Mas, A. D. King, R. P. Wayne and M. R. Wilson, *J. Chem. Soc., Faraday Trans*, 1991, **87**, 2913-2919.
6. D. Burgess, NIST Chemistry WebBook, NIST Standard Reference Database Number 69, *National Institute of Standards and Technology*, 2018, https://doi.org/10.18434/T4D303.
7. R. R. Baldwin, G. R. Drewery and R. W. Walker, *J. Chem. Soc., Faraday Trans 1: Physical Chemistry in Condensed Phases*, 1984, **80**, 3195-3207.
8. L. Zhou, A. R. Ravishankara, S. S. Brown, M. Idir, K. J. Zarzana, V. Daële and A. Mellouki, *J. Phys. Chem. A*, 2017, **121**, 4464-4474.
9. F. Bernard, G. Eyglunent, V. Daele and A. Mellouki, *J. Phys. Chem. A*, 2010, **114**, 8376-8383.
10. H. Chen, Y. Ren, M. Cazaunau, V. Dalele, Y. Hu, J. Chen and A. Mellouki, *Chem. Phys. Lett.*, 2015, **621**, 71-77.
11. S. S. Brown, H. Stark and A. R. Ravishankara, *Appl. Phys. B-lasers. O*, 2002, **75**, 173-182.

12. S. S. Brown, H. Stark, S. J. Ciciora, R. J. McLaughlin and A. R. Ravishankara, *Rev. Sci. Instrum.*, 2002, **73**, 3291-3301.

13. S. S. Brown, *Chem. Rev.*, 2003, **103**, 5219-5238.

14. N. L. Wagner, W. P. Dube, R. A. Washenfelder, C. J. Young, I. B. Pollack, T. B. Ryerson and S. S. Brown, *Atmos. Meas. Tech.*, 2011, **4**, 1227-1240.

15. H. Fuchs, W. P. Dube, S. J. Cicioira and S. S. Brown, *Anal. Chem.*, 2008, **80**, 6010-6017.

16. W. P. Dube, S. S. Brown, H. D. Osthoff, M. R. Nunley, S. J. Ciciora, M. W. Paris, R. J. McLaughlin and A. R. Ravishankara, *Rev. Sci. Instrum.*, 2006, **77**.

17. H. Fuchs, W. R. Simpson, R. L. Apodaca, T. Brauers, R. C. Cohen, J. N. Crowley, H. P. Dorn, W. P. Dubé, J. L. Fry, R. Häseler, Y. Kajii, A. Kiendler-Scharr, I. Labazan, J. Matsumoto, T. F. Mentel, Y. Nakashima, F. Rohrer, A. W. Rollins, G. Schuster, R. Tillmann, A. Wahner, P. J. Wooldridge and S. S. Brown, *Atmos. Meas. Tech.*, 2012, **5**, 2763-2777.

18. H. P. Dorn, R. L. Apodaca, S. M. Ball, T. Brauers, S. S. Brown, J. N. Crowley, W. P. Dube, H. Fuchs, R. Haeseler, U. Heitmann, R. L. Jones, A. Kiendler-Scharr, I. Labazan, J. M. Langridge, J. Meinen, T. F. Mentel, U. Platt, D. Poehler, F. Rohrer, A. A. Ruth, E. Schlosser, G. Schuster, A. J. L. Shillings, W. R. Simpson, J. Thieser, R. Tillmann, R. Varma, D. S. Venables and A. Wahner, *Atmos. Meas. Tech.*, 2013, **6**, 1111-1140.

19. P. L. Kebabian, E. C. Wood, S. C. Herndon and A. Freedman, *Environ Sci Technol*, 2008, **42**, 6040-6045.

20. J. A. Davidson, A. A. Viggiano, C. J. Howard, I. Dotan, F. C. Fehsenfeld, D. L. Albritton and E. E. Ferguson, *J. Chem. Phys.*, 1978, **68**, 2085-2087.

21. J. Burkholder, S. Sander, J. Abbatt, J. Barker, R. Huie, C. Kolb, M. Kurylo, V. Orkin, D. Wilmouth and P. Wine, "Chemical Kinetics and Photochemical Data for Use in Atmospheric Studies, Evaluation No. 18," JPL Publication 15-10, Jet Propulsion Laboratory, Pasadena, 2015 http://jpldataeval.jpl.nasa.gov.

22. R. Atkinson, D. L. Baulch, R. A. Cox, J. N. Crowley, R. F. Hampson, R. G. Hynes, M. E. Jenkin, M. J. Rossi and J. Troe, *Atmos. Chem. Phys.*, 2004, **4**, 1461-1738.

23. V. Daele, G. Laverdet, G. Le Bras and G. Poulet, *J. Phys. Chem.*, 1995, **99**, 1470-1477.

24. A. Ray, V. Daële, I. Vassalli, G. Poulet and G. Le Bras, *J. Phys. Chem.*, 1996, **100**, 5737-5744.

25. S. Vaughan, C. E. Canosa-Mas, C. Pfrang, D. E. Shallcross, L. Watson and R. P. Wayne, *Phys Chem Chem Phys*, 2006, **8**, 3749-3760.

26. R. Atkinson, D. L. Baulch, R. A. Cox, J. N. Crowley, R. F. Hampson, R. G. Hynes, M. E. Jenkin, M. J. Rossi, J. Troe and I. Subcommittee, *Atmos Chem Phys*, 2006, **6**, 3625-4055.

27. M. E. Jenkin, S. M. Saunders and M. J. Pilling, *Atmos. Environ.*, 1997, **31**, 81-104.

28. J. P. Burrows, G. S. Tyndall and G. K. Moortgat, *J. Phys. Chem.*, 1985, **89**, 4848-4856.

29. T. J. Wallington, R. Atkinson, A. M. Winer and J. N. Pitts, *J. Phys. Chem.*, 1986, **90**, 4640-4644.

30. C. A. Cantrell, J. A. Davidson, R. E. Shetter, B. A. Anderson and J. G. Calvert, *J. Phys. Chem.*, 1987, **91**, 6017-6021.

31. A. L. Castelhano and D. Griller, *J. Am. Chem. Soc.*, 1982, **104**, 3655-3659.

32. B. S. Rabinovitch and D. W. Setser, eds W. A. Noyes, G. S. Hammond and J. N. Pitts, *in Advances in Photochemistry,* 2007, doi:10.1002/9780470133330.ch1.

33. J. C. Nesheim and J. D. Lipscomb, *Biochemistry-us.*, 1996, **35**, 10240-10247.

34. S. S. Brown and J. Stutz, *Chem. Soc. Rev.*, 2012, **41**, 6405-6447.

35. R. Atkinson and J. Arey, *Chem. Rev.*, 2003, **103**, 4605-4638.

36. O. W. Wingenter, M. K. Kubo, N. J. Blake, T. W. Smith, D. R. Blake and F. S. Rowland, *J. Geophys. Res.: Atmos.*, 1996, **101**, 4331-4340.

37. N. Carslaw, L. Carpenter, J. Plane, B. Allan, R. Burgess, K. Clemitshaw, H. Coe and S. Penkett, *J. Geophys. Res.: Atmos.*, 1997, **102**, 18917-18933.

Figures

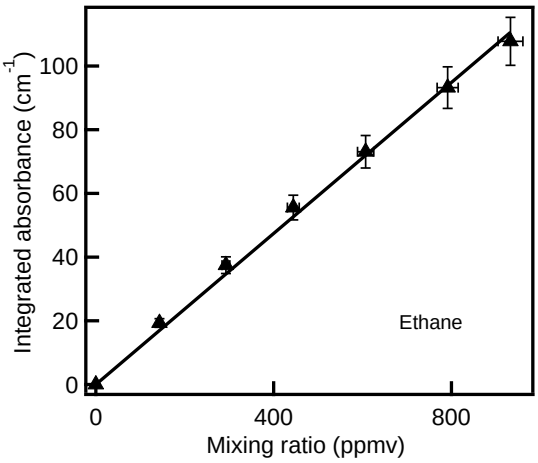

Figure 1. Calibration curve for ethane- A plot of the integrated absorbance of ethane centered at 837 cm^{-1} (measured as the area under the absorbance between 940-734 cm^{-1}) as a function of the mixing ratio of ethane in the chamber as determined by manometric measurements. The data was fit to a line passing through zero using a linear least-squares analysis. The uncertainties in each point, derived from multiple measurements, are shown as vertical error bars.

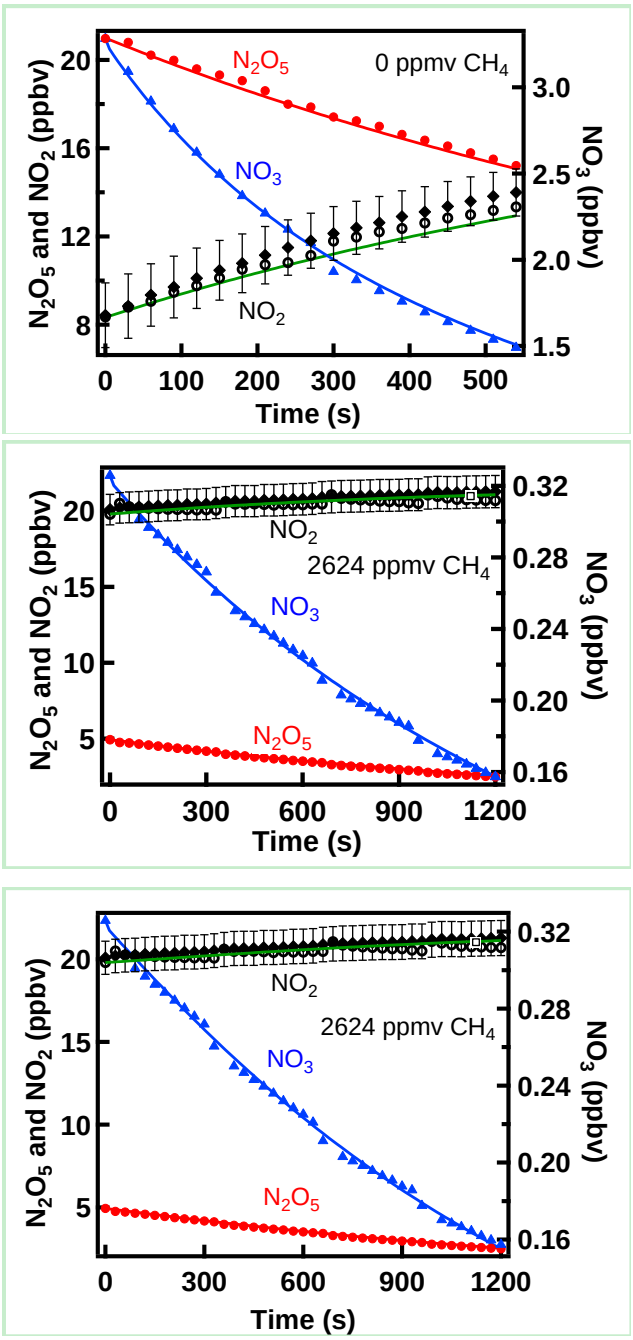

Figure 2. Observed (data points) and simulated (lines) profiles of N_2O_5, NO_3 and NO_2 as a function of time. Mixing ratios of CH_4 are shown in each panel. The simulations in the middle panel did not include secondary reactions of NO_3 reaction products while those in the bottom panel included such reactions (shown in Table 1).

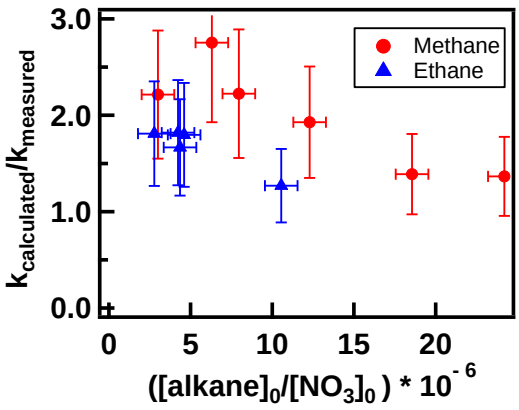

Figure 3 The ratio of calculated rate coefficients to that measured without accounting for secondary reactions (Ratio 1) versus the ratio of alkanes to NO_3 (Ratio 2) for reactions (1) and (2). Clearly, the ratio approaches 1.0 as Ratio 2 increases.

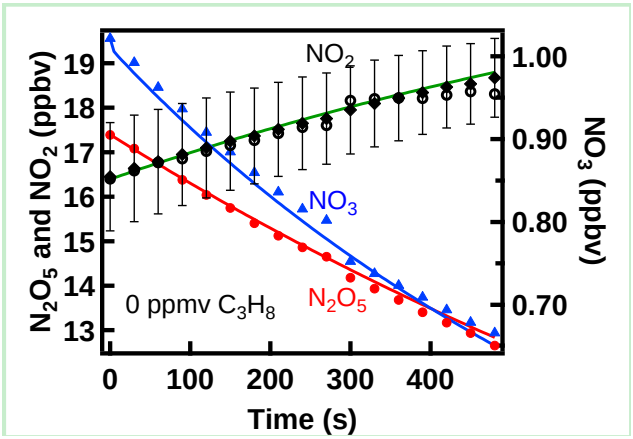
NO2
NO3
N2O5
0 ppmv C3H8
N2O5 and NO2 (ppbv)
NO3 (ppbv)
Time (s)

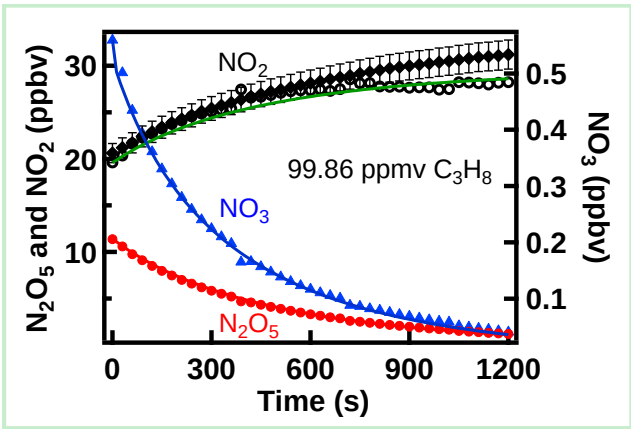
NO2
NO3
N2O5
99.86 ppmv C3H8
N2O5 and NO2 (ppbv)
NO3 (ppbv)
Time (s)

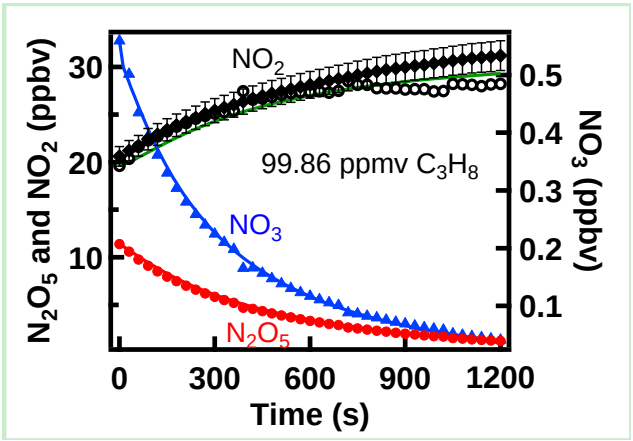
NO2
NO3
N2O5
99.86 ppmv C3H8
N2O5 and NO2 (ppbv)
NO3 (ppbv)
Time (s)

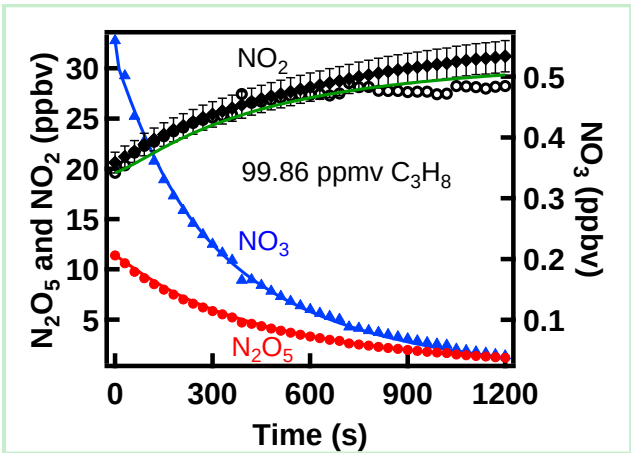
NO2
NO3
N2O5
99.86 ppmv C3H8
N2O5 and NO2 (ppbv)
NO3 (ppbv)
Time (s)

Figure 4. Observed (data points) and simulated (lines) profiles of N_2O_5, NO_3 and NO_2 as a function of time. Mixing ratios of propane (C_3H_8) are shown in each panel. The simulations in the 2nd panel did not include secondary reactions of NO_3 reaction products while those in the 3rd panel included such reactions (shown in Table 1). The simulations in the 4th panel included both secondary reactions and reactions with impurities (see Table S1).

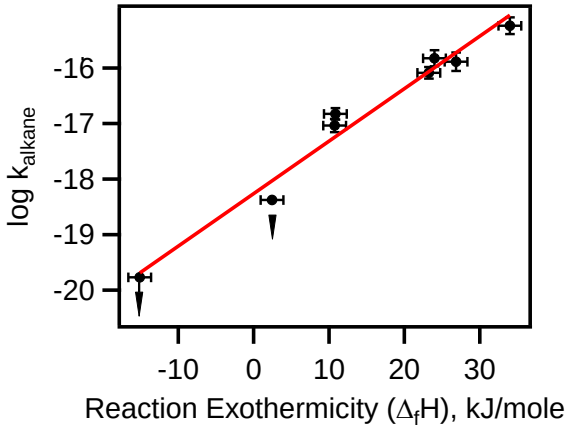

Figure 5: Rate coefficient for the reaction of NO_3 with alkanes on a logarithm scale plotted against the exothermicity for each reaction shown in the text. The upper limits for reactions with methane and ethane are shown with arrows to highlight that they are upper limits. Note, the slope of the plot would be larger if the rate coefficients for NO_3 reactions with methane and ethane were lower than indicated.

Tables

Table 1. Reactions of the products of the NO_3 reaction with alkanes in the presence of O_2 and nitrogen oxides included in simulating the temporal profiles of NO_3 and N_2O_5.

Reaction	Rate coefficients 298 K, 1 bar air (cm^3 $molecule^{-1}s^{-1}$ or s^{-1})	Reference
alkane $+NO_3 \xrightarrow{k_x} R_1 + HNO_3$	k_x (k_1-k_8)	This work
$N_2O_5 \xrightarrow{k_9} NO_3 + NO_2$	0.0369	a
$NO_3 + NO_2 \xrightarrow{k_{10}} N_2O_5$	1.35×10^{-12}	a
$NO_3 \xrightarrow{k_{11}}$ loss	k_{11}	b
$N_2O_5 \xrightarrow{k_{12}}$ loss	k_{12}	b
$R_1 + O_2 \xrightarrow{k_{13}} R_1O_2$	10^{-11}	c
$R_1O_2 + NO_3 \xrightarrow{k_{14}} R_1O + NO_2$		
R_1: CH_3	1.2×10^{-12}	d
R_1: C_2H_5 and other alkyl radical	2.3×10^{-12}	e
$R_1O_2 + R_1O_2 \xrightarrow{k_{15}} 2R_1O$		
R_1: CH_3	3.5×10^{-13}	f
R_1: C_2H_5	7.6×10^{-14}	f
R_1: n-C_3H_7	3×10^{-13}	f
R_1: i-C_3H_7	1×10^{-15}	f
R_1: s-C_4H_9	2.5×10^{-13}	g
R_1: t-C_4H_9	6.7×10^{-15}	g
R_1: cycle-C_6H_5	2.5×10^{-13}	g
$R_1O_2 + NO_2 \xrightarrow{k_{16}} R_1O_2NO_2$		
R_1: CH_3	4.0×10^{-12}	c
R_1: C_2H_5 and other alkyl radical	5.1×10^{-12}	c
$R_1O_2NO_2 \xrightarrow{k_{17}} R_1O_2 + NO_2$		
R_1: CH_3	1.5	c

R_1: C_2H_5 and other alkyl radical	3.4	c
$R_1O + O_2 \xrightarrow{k_{18}} R_2CHO + HO_2$	7.14×10^{-14}	g
$R_1O_2 + HO_2 \xrightarrow{k_{19}} R_1OOH + O_2$		
R_1: CH_3	5.2×10^{-12}	f
R_1: C_2H_5	7.97×10^{-12}	g
R_1: i-C_3H_7	1.19×10^{-11}	g
R_1: s-C_4H_9	1.43×10^{-11}	g
R_1: t-C_4H_9	1.43×10^{-11}	g
R_1: C_6H_{13}	1.76×10^{-11}	g
R_1: cycle-C_6H_{11}	1.76×10^{-11}	g
$R_2CHO + NO_3 \xrightarrow{k_{20}} R_3COOO + HNO_3$		
R_3: H	5.5×10^{-16}	f
R_3: CH_3 and other alkyl radical	2.7×10^{-15}	f
$HO_2 + NO_3 \xrightarrow{k_{21}} OH + NO_2 + O_2$	4×10^{-12}	f
$OH + NO_3 \xrightarrow{k_{22}} HO_2 + NO_2$	2×10^{-11}	f
$NO_2 + OH \xrightarrow{k_{23}} HONO_2$ / HOONO	6.5×10^{-11}	f

a ([21])

b (Derived from the first period of the experiments: observation in the absence of alkanes)

c ([22])

d ([23])

e ([24, 25])

f ([26])

g ([27])

Table 2. Summary of the experimental conditions and upper limits for reaction of NO_3 with methane and ethane at 298.0±1.5K.

Compound	Initial mixing ratio				$k_{alkane1}$ [a]	$k_{alkane2}$ [b]
	Alkane (ppmv)	NO_3 (ppbv)	N_2O_5 (ppbv)	NO_2 (ppbv)	(cm^3 $molecule^{-1}s^{-1}$)	
Methane	2624	0.33	4.93	19.80	2.98×10^{-20}	1.34×10^{-20}
	2520	0.84	14.49	22.49	2.48×10^{-20}	1.12×10^{-20}
	2598	0.14	2.22	20.93	3.68×10^{-20}	2.65×10^{-20}
	3440	0.28	5.14	19.11	1.55×10^{-20}	8.04×10^{-21}
	3276	0.52	10.38	20.59	1.90×10^{-20}	6.90×10^{-21}
	3389	0.14	2.64	19.33	2.80×10^{-20}	2.05×10^{-20}
				Average	$(2.5\pm1.7)\times10^{-20}$	$(1.7\pm1.5)\times10^{-20}$
Ethane	958	0.22	4.84	26.63	7.50×10^{-19}	4.50×10^{-19}
	1106	0.24	5.74	23.25	7.60×10^{-19}	4.23×10^{-19}
	1095	0.09	2.46	25.88	6.01×10^{-19}	4.30×10^{-19}
	1101	0.26	6.57	23.60	7.37×10^{-19}	4.05×10^{-19}
	1000	0.36	10.24	26.41	7.13×10^{-19}	3.94×10^{-19}
	1055	0.10	2.84	26.05	6.37×10^{-19}	5.02×10^{-19}
				Average	$(7.1\pm1.3)\times10^{-19}$	$(4.2\pm0.4)\times10^{-19}$

[a] The calculated value without including secondary reactions shown in Table 1. Quoted errors are at the 95% confidence level and are measures of the precision of our measurements. It includes Student t-distribution contribution due to the limited number of measurements.

[b] The calculated values that include secondary reactions shown in Table 1. Quoted errors are at the 95% confidence level and are measures of the precision of our measurements. It includes Student t-distribution contribution due to the limited number of measurements.

Table 3. Summary of the experimental conditions and rate coefficients for reaction of NO_3 with propane, n-butane, iso-butane, 2,3-dimethylbutane cyclopentane and cyclohexane at 298.0±1.5K.

Compound	Initial mixing ratio of reactants in the chamber				$k_{alkane1}$ [a]	$k_{alkane2}$ [b]	k_{alkane} [c] incl. systematic errors
	Alkane (ppmv)	NO_3 (ppbv)	N_2O_5 (ppbv)	NO_2 (ppbv)	(cm^3 $molecule^{-1}s^{-1}$)		
propane	99.86	0.56	11.38	19.61	1.73×10^{-17}	9.40×10^{-18}	
	60.81	0.72	12.10	20.43	1.80×10^{-17}	1.02×10^{-17}	
	51.08	0.85	15.56	16.27	1.68×10^{-17}	9.38×10^{-18}	
	98.39	0.10	2.88	27.49	1.27×10^{-17}	1.01×10^{-17}	
	59.62	0.10	2.40	29.07	1.23×10^{-17}	9.12×10^{-18}	
				Mean average	$(1.5\pm0.6)\times10^{-17}$	$(9.2\pm2.1)\times10^{-18}$	$(9.2\pm2.9)\times10^{-18}$
n-butane	19.72	1.03	18.26	18.13	3.10×10^{-17}	1.35×10^{-17}	
	18.70	0.14	3.80	28.22	2.42×10^{-17}	1.59×10^{-17}	
	30.78	1.06	18.10	15.16	3.10×10^{-17}	1.65×10^{-17}	
	29.68	0.12	3.33	25.55	2.24×10^{-17}	1.56×10^{-17}	
	24.26	0.79	11.05	14.24	3.60×10^{-17}	1.56×10^{-17}	
				Mean average	$(2.9\pm1.1)\times10^{-17}$	$(1.5\pm0.2)\times10^{-17}$	$(1.5\pm0.4)\times10^{-17}$
iso-butane	13.90	0.83	9.40	12.99	1.35×10^{-16}	8.57×10^{-17}	
	13.73	0.10	1.86	21.23	8.93×10^{-17}	7.43×10^{-17}	
	10.26	1.10	14.64	13.84	1.40×10^{-16}	8.21×10^{-17}	
	10.04	0.10	2.42	25.26	9.52×10^{-17}	7.67×10^{-17}	
	5.22	1.30	14.04	12.07	1.65×10^{-16}	9.00×10^{-17}	
				Mean average	$(1.3\pm0.6)\times10^{-16}$	$(8.2\pm1.3)\times10^{-17}$	$(8.2\pm2.2)\times10^{-17}$
2,3-dimethyl butane	1.02	0.25	3.90	19.41	1.55×10^{-15}	6.80×10^{-16}	
	0.51	0.23	5.50	24.05	1.00×10^{-15}	5.50×10^{-16}	
	0.38	0.58	9.57	18.17	1.25×10^{-15}	6.32×10^{-16}	
	0.38	0.12	2.56	23.80	7.84×10^{-16}	5.44×10^{-16}	
	0.26	0.64	9.20	14.47	1.25×10^{-15}	6.02×10^{-16}	
	0.24	0.10	2.09	20.27	7.03×10^{-16}	4.82×10^{-16}	
				Mean average	$(1.1\pm0.6)\times10^{-15}$	$(5.8\pm1.4)\times10^{-16}$	$(5.8\pm2.4)\times10^{-16}$

cyclopentane	1.76	0.72	8.59	13.33	3.50×10^{-16}	1.80×10^{-16}	
	1.41	0.24	3.91	17.98	3.20×10^{-16}	1.68×10^{-16}	
	2.04	0.57	10.66	19.67	2.70×10^{-16}	1.31×10^{-16}	
	1.71	0.19	4.26	23.97	2.60×10^{-16}	1.38×10^{-16}	
	2.04	0.11	2.49	24.61	1.99×10^{-16}	1.41×10^{-16}	
	1.78	0.63	9.39	17.14	2.60×10^{-16}	1.29×10^{-16}	
	1.71	0.10	2.10	23.84	1.96×10^{-16}	1.41×10^{-16}	
				Mean average	$(2.6\pm1.1)\times10^{-16}$	$(1.5\pm0.4)\times10^{-16}$	$(1.5\pm0.6)\times10^{-16}$
cyclohexane	2.51	0.39	7.73	22.05	2.30×10^{-16}	1.20×10^{-16}	
	1.88	0.45	7.89	19.40	2.35×10^{-16}	1.34×10^{-16}	
	1.82	0.10	2.16	24.09	1.98×10^{-16}	1.41×10^{-16}	
	1.54	0.46	6.85	16.70	2.50×10^{-16}	1.27×10^{-16}	
	1.50	0.11	2.04	20.55	1.92×10^{-16}	1.39×10^{-16}	
	1.98	0.50	10.42	21.08	2.30×10^{-16}	1.12×10^{-16}	
				Mean average	$(2.2\pm0.5)\times10^{-16}$	$(1.3\pm0.3)\times10^{-16}$	$(1.3\pm0.4)\times10^{-16}$

[a] The calculated values do not account for the secondary reactions listed in Table 1. Quoted errors are at the 95% confidence level and are measures of the precision of our measurements. It includes Student t-distribution contribution due to the limited number of measurements.

[b] The calculated values include accounting for secondary reactions listed in Table 1. Quoted errors are at the 95% confidence level and are measures of the precision of our measurements. It includes Student t-distribution contribution due to the limited number of measurements.

[c]The quoted errors include estimated systematic errors as described in the text.

Table 4. Summary of literature values for the rate coefficients of NO_3 radicals with alkanes at room temperature compared with those from this study.

Reactant	k_{alkane} reported $10^{-17}cm^3$ $molecule^{-1}s^{-1}$	Technique	Reference
Methane	≤40	Absolute method	[28]
	≤2	Absolute method	[29]
	≤0.0004	Indirect*	[30]
	≤0.08	Absolute method	[5]
	≤0.004	Absolute method	This work(k_1)
Ethane	≤0.4	Absolute method	[29]
	0.2	Indirect**	[4]
	≤(2.7±0.2)	Absolute method	[5]
	<0.05	Absolute method	This work(k_2)
Propane	≤(4.8±1.7)	Absolute method	[5]
	0.92±0.29	Absolute method	This work(k_3)
n-butane	7.5±1.9	Relative method (ethene)[a]	[2]
	≤2	Absolute method	[29]
	4.5±0.6	Absolute method	[4]
	1.5±0.4	Absolute method	This work(k_4)
iso-butane	11.2±2.8	Relative method (ethene)[a]	[2]
	11±2	Absolute method	[4]
	≤(60±10)	Absolute method	[5]
	8.2±2.2	Absolute method	This work(k_5)
	10.1±1.3	Weighted average	
2,3-dimethylbutane	46.2±11.5	Relative method (ethene)[a]	[2]
	40.6±5.7	Relative method (trans-2-butene)[b]	[3]
	58±24	Absolute method	This work(k_6)
	42.4±5.0	Weighted average	
cyclopentane	15±6	Absolute method	This work(k_7)
cyclohexane	19.0±9.0	Relative method (2,3-dimethylbutane)[c]	[2]
	13±4	Absolute method	This work(k_8)
	14.0±3.7	Weighted average	

[a] The values from the literatures were recalculated by using the rate constant of ethene with NO_3 to be (2.4± 0.6) × 10^{-16} cm^3 $molecule^{-1}$ s^{-1}, which was measured here using the absolute method.

[b] The rate constant of trans-2-butene (reference compound) with NO_3 radicals was (3.87 ±0.45) ×$10^{-13}$$cm^3$ $molecule^{-1}s^{-1}$.

[c] The values from the literatures were recalculated by using the rate constant of 2,3-dimethylbutane with NO_3 to be (5.8 ± 2.4) × 10^{-16} cm^3 $molecule^{-1}$ s^{-1} obtained in this work.

*Estimated based on the absence of CO and CO_2 formation.

** The rate coefficient at room temperature assuming k_{ethane} = 2.0 × 10^{-18} cm^3 $molecule^{-1}s^{-1}$ and via an Arrhenius extrapolation to 298 K.

Table 5. Summary of the experimental conditions and rate coefficients for the reactions of NO_3 with n-butane-d10 and n-butane-d6 at 298.0±1.5K.

Compound	Initial mixing ratio of reactants in the chamber				$k_{alkane1}$ [a]	$k_{alkane2}$ [b]	k_{alkane} [c] incl. systematic errors
	VOC (ppmv)	NO_3 (ppbv)	N_2O_5 (ppbv)	NO_2 (ppbv)	(cm^3 $molecule^{-1}s^{-1}$)		
n-butane -d10	52.43	0.56	13.38	22.55	1.28×10^{-17}	6.31×10^{-18}	
	50.21	0.13	3.75	28.38	1.08×10^{-17}	6.89×10^{-18}	
	30.60	1.07	14.05	14.09	1.62×10^{-17}	7.98×10^{-18}	
	29.03	0.15	3.21	22.86	1.41×10^{-17}	8.56×10^{-18}	
	32.69	0.21	7.52	23.93	1.50×10^{-17}	8.62×10^{-18}	
	31.07	0.14	5.27	25.32	1.31×10^{-17}	7.78×10^{-18}	
				Mean average	$(1.4\pm0.4)\times10^{-17}$	$(7.4\pm2.0)\times10^{-18}$	$(7.4\pm2.3)\times10^{-18}$
n-butane -d6	11.05	0.08	3.85	28.14	2.12×10^{-17}	1.81×10^{-17}	
	11.00	0.26	11.63	26.47	3.92×10^{-17}	1.97×10^{-17}	
	10.05	0.10	5.21	29.59	3.64×10^{-17}	2.19×10^{-17}	
				Mean average	$(3.2\pm1.9)\times10^{-17}$	$(2.0\pm0.4)\times10^{-18}$	$(2.0\pm0.5)\times10^{-18}$

[a] The calculated values without accounting for secondary reactions shown in Table 1. Quoted errors are at the 95% confidence level and are measures of the precision of our measurements. It includes Student t-distribution contribution due to the limited number of measurements.

[b] The calculated values accounting for secondary reactions shown in Table 1. Quoted errors are at the 95% confidence level and are measures of the precision of our measurements. It includes Student t-distribution contribution due to the limited number of measurements.

[c]The quoted errors include estimated systematic errors as described in the text.